Fuel 276 (2020) 118031

Contents lists available at ScienceDirect

Fuel

journal homepage: www.elsevier.com/locate/fuel

Full Length Article

Oil recovery from fractured porous media with/without initial water saturation by using 3-pentanone and its aqueous solution

Francisco J. Argüelles-Vivas, Mingyuan Wang, Gayan A. Abeykoon, Ryosuke Okuno*

Hildebrand Department of Petroleum and Geosystems Engineering, The University of Texas at Austin, 200 E. Dean Keeton Street, Stop C0300, Austin, TX 78712, USA

ARTICLE INFO

Keywords:
Ketone solvent
Wettability alteration
3-pentanone
Imbibition
Improved oil recovery
Initial water saturation

ABSTRACT

This paper presents an application of 3-pentanone, a symmetric dialkyl ketone, to enhance the water imbibition in coreflooding of fractured carbonate cores. 3-Pentanone was tested in two ways: 1.1- wt% 3-pentanone solution in reservoir brine (3pRB) and pure 3-pentanone (3p) as a miscible solvent. It was presented previously that 3p is a mutual solvent for oil and water, and can rapidly change the rock wettability to strongly water-wet with its electron-rich oxygen atom through the oil and water phases. The main objective of this research is to investigate how the initial water saturation (S_{wi}) in the matrix affects the imbibition of 3pRB or 3p from the fracture and the resulting recovery of oil from the matrix.

The experimental results were analyzed in terms of material balance (mass and volume) with simplifying assumptions. This analysis enabled to estimate how much of the injected components were imbibed into the surrounding matrices from the fracture and the relative contribution of the injected components to displacing oil in the matrix. Results for the 3pRB and 3p injections indicate collectively that 3-pentanone was more effective in enhancing oil recovery when an aqueous phase was initially present in the matrix.

1. Introduction

Hydraulic fracturing made possible the recovery of oil from shales at economically feasible production rates. However, the petrophysical properties of shales, such as ultra-low permeability, heterogeneous mineralogy, and high total organic content (TOC), result in recovery factors typically below 10% [1,2]. The presence of organic matter and the high content of calcite and dolomite tend to cause the shales to be oil-wet or mixed-wet.

Surfactant solutions have been proposed to facilitate the imbibition of water into the shale matrix and thus enhance oil production [3–6]. The recovery mechanisms of surfactants are the rock-wettability change toward a more water-wet state and the reduction of interfacial tension (IFT) between the aqueous and oleic phases [7–16].

Cationic, anionic and non-ionic surfactants have been investigated to evaluate their performance in shales. For example, Alvarez et al. tested anionic and non-ionic surfactants on carbonate and siliceous shales to modify the wettability from oil-wet to water-wet [10]. They found that the anionic surfactant was a better wettability modifier than the non-ionic surfactant. Liu et al. showed that anionic surfactants altered the wettability of siliceous shales, while non-ionic surfactants did not affect the wettability [14]. Alvarez et al. and Alvarez and Schechter have pointed out that IFT should not be decreased to ultralow values (10^{-3} mN/m) during the application of surfactants in shales [4,6] because the enhancement of water imbibition does not require ultra-low IFT. This is different from the conventional application of surfactant solutions for tertiary oil recovery, in which ultra-low IFT is required for coalescence of oil droplets during the displacement of oil by an optimized surfactant formulation [16]. Kathel and Mohanty found that surfactant imbibition rate and oil recovery were lower with lower IFT in experiments with tight sandstones [9]. In fractured carbonates, Adibhatla and Mohanty observed that oil-recovery rate diminished with decreasing IFT for surfactant solutions that changed wettability toward a water-wet state [15]. These results indicate that the expected mechanism of surfactant solution for enhancing the water imbibition into the matrix might not be optimized with ultra-low IFT.

Recently, Wang et al. [17] investigated the application of 3-pentanone as an additive to reservoir brine (RB) that enhances oil recovery from oil-wet or mixed-wet cores. 3-Pentanone is a symmetric dialkyl ketone that partitions into oil and water at reservoir conditions. It is a colorless liquid at standard conditions, widely used in the food industry, non-toxic and available at low-cost. 3-Pentanone was tested as a novel chemical that works as a wettability modifier without changing the water/oil IFT and also as a miscible solvent to oil at reservoir conditions. Spontaneous and forced imbibition experiments were performed with oil-wet limestone cores and RB and 3pRB. Their results indicated

* Corresponding author.
E-mail address: okuno@utexas.edu (R. Okuno).

https://doi.org/10.1016/j.fuel.2020.118031
Received 19 March 2020; Received in revised form 2 May 2020; Accepted 5 May 2020
Available online 15 May 2020
0016-2361/

that 3-pentanone improves oil recovery by wettability alteration, and also by oil swelling and viscosity reduction, as a consequence of the miscibility of 3-pentanone with oil.

Wang et al. [18] compared the performance of 3-pentanone and a non-ionic surfactant as additives to RB to enhance the water imbibition from a fracture into the surrounding matrices. Coreflooding experiments in fractured cores showed that 3pRB recovered oil more rapidly than the surfactant solution by spontaneous imbibition. They confirmed 3pRB did not change the original water/oil IFT, which favorably increased the capillary force to accelerate the water imbibition by wettability alteration.

Overall, Wang et al. showed that 3-pentanone is a promising chemical to recover oil from oil-wet fractured formations, such as shales and tight carbonates [17,18]. However, it is unknown how S_{wi} would affect the performance of 3-pentanone or 3pRB. Water saturations in shale plays can be high after their primary depletion; e.g., the water-cut was reported to be 90% in part of the Permian basin [19].

It is extensively investigated for conventional reservoirs that initial water saturation (S_{wi}) influences the spontaneous imbibition rate and oil recovery [20–25]. However, the results from these investigations are not consistent regarding how S_{wi} affects the performance of water imbibition. Viksund et al. observed that the final oil recovery factor in Berea sandstones by spontaneous water imbibition was little affected by the initial water saturation in the range from 0 to 30%. Imbibition rate decreased as S_{wi} increased in the range of 0 to 6%, and then it increased as S_{wi} increased from 15 to 34%. For chalk cores, Viksund et al. found a greater variation in oil recovery. For Rørdal chalks, the oil recovery decreased from 67 to 30% as the S_{wi} increased from 7.5% to 51%. The imbibition rate first increased with the augmentation of S_{wi} up to 34%, and then it slightly decreased [20]. By countercurrent spontaneous imbibition experiments in Berea sandstones, Cil et al. found that the initial water saturation in the range of 0 to 20% did not affect the oil recovery significantly. Above 20% of S_{wi}, the oil recovery increased [21].

Zhou et al. investigated the relationship among rock wettability, S_{wi}, aging time, and oil recovery during spontaneous imbibition and waterflooding on Berea sandstone. They found that the imbibition rate and final oil recovery decreased as the initial water saturation decreased (as a consequence of larger aging time and less water wetness) [22]. Akin et al. performed imbibition experiments with diatomite cores. Their results showed that oil recovery decreased as S_{wi} increased (up to 60%). They also observed that residual oil saturation was not greatly affected by S_{wi} (recovery was measured in the unit of pore volume) [23].

Tong et al. found no systematic effect of S_{wi} on oil recovery with Berea sandstones. After scaling to reservoir conditions, they found that oil recovery was sensitive to S_{wi}. It increased as S_{wi} increased within the range of 11–28% [24]. Li and Li numerically investigated the effects of S_{wi} on oil recovery by imbibition. They found that S_{wi} did not affect the recoverable oil at a reservoir scale. They also observed no change in oil production rate at the reservoir scale, unlike in core-scale experiments. They explained that this difference was because the displacement was forced imbibition at the reservoir scale, whereas it was spontaneous imbibition at the core scale [25].

There are a limited number of studies for the effects of S_{wi} on water imbibition in shales [26,27]. S_{wi} has been reported to be 25% for organic Barnett shale [28], and 20% for Horn River shale [27]. For Otter Park and Evie gas shales, Ghanbari and Dehghanpour found that S_{wi} decreased the water imbibition rate, but S_{wi} did not affect the oil imbibition rate. They also stated that hydrophobic organic material could diminish the water imbibition rate [26]. Gao and Hu studied the effects of S_{wi} and imbibing fluid on the spontaneous imbibition into Barnett shale cores. Their results showed that S_{wi} affected spontaneous imbibition into shales, but the effects depended on mineral composition. They pointed out that the high heterogeneity of shales made the imbibition process complicated and, therefore, each shale type needed a specific study [27].

The main objective of this research was to study the effects of S_{wi} on the imbibition of water and 3-pentanone into fractured cores. This question is important particularly because shale oil reservoirs show large watercuts. Two injection schemes were considered for water imbibition enhancement by 3-pentanone in the presence of S_{wi}. For the first scheme, 3-pentanone was used as 3pRB to enhance the water imbibition with cores #1 ($S_{wi} = 0$) and #2 ($S_{wi} = 0.311$). For the second scheme, 3-pentanone was injected as a pure solvent with cores #3 ($S_{wi} = 0$) and #4 ($S_{wi} = 0.28$). These four coreflooding experiments were analyzed by compositional material balance, which quantitatively showed the effect of S_{wi} on oil recovery by 3-pentanone, either as 3pRB or pure 3p.

Section 2 presents the materials and methods for this research. Section 3 presents the main results of the coreflooding experiments. Section 4 gives a summary and conclusions from this research.

2. Materials and methods

This section presents the materials and methods for the current study. Relevant information regarding 3-pentanone was taken from Wang et al. [17,18]. A complete set of experimental data for 3-pentanone and its mixtures with oil and reservoir brine (RB) can be found in their original paper.

2.1. Reservoir fluid properties

A sample of crude oil from an oil reservoir in Texas was used for the experiments. The experimental temperature is 347 K. Table 1 shows the pertinent properties of the oil sample for this study. This oil is more viscous than the oil studied by Wang et al. [17,18]. RB with a salinity of 68722 ppm was prepared based on accessible field data (Table 2). The density of RB was 1030 kg/m^3 at 347 K and atmospheric pressure.

2.2. 3-Pentanone properties

3-Pentanone (purity > 99%) was obtained from Sigma-Aldrich. The density of 3-pentanone is 760 kg/m^3 at 347 K and atmospheric pressure [29]. Aqueous stability of 3-pentanone in RB, wettability measurements with calcite surfaces, and oil dilution by 3-pentanone were reported by Wang et al. [17].

The concentration of 3-pentanone in RB used in this research is 1.1 wt%, which is the solubility limit of 3-pentanone in RB at 347 K. This aqueous solution is referred to as “3pRB” in this paper. The density of 3pRB was 1030 kg/m^3 at 347 K and atmospheric pressure.

Wang et al. demonstrated that 3-pentanone modifies the wettability of calcite from oil-wet to water-wet. The average contact angle of oil droplets on oil-aged calcite surfaces in 3pRB decreased from 95° to 74° within two hours, and further decreased to 26° after 66 h [17]. None of the oil droplets was attached on the calcite surface after 3 days. An IFT experiment showed that 3pRB did not affect the IFT between the crude oil and RB (approximately 11 mN/m) [17].

Table 1
Properties of the crude oil sample used in this research.

Molecular weight, g/mol		210
Density, kg/m^3		878 (at 293 K) 849.6 (at 347 K)
Viscosity, cP		2.6 (at 347 K)
SARA, wt%	Saturates	71.6
	Aromatics	24.8
	Resins	3.0
	Asphaltenes (pentane insoluble)	< 0.1

Table 2
Composition of the reservoir brine (RB) used in this research (68722 ppm). The density of RB was 1030 kg/m^3 at 347 K and atmospheric pressure.

Cations	ppm	Anions	ppm
Na^+	25,170	Cl^-	41,756
K^+	210	SO_4^{2-}	108
Ca^{2+}	1292		
Mg^{2+}	187		
Sum	26858.24	Sum	41863.73

2.3. Experimental procedure for coreflooding

Four Texas cream limestone cores were prepared for coreflooding experiments. They have a diameter of 0.0254 m and a length of 0.229 m. Cores #1 and #3 were fully saturated with oil, and cores #2 and #4 with RB first and then with oil at 347 K and atmospheric pressure. The porosities, permeabilities and water and oil saturations were measured for all cores. Then, the cores were placed in a container filled with oil for at least one month at 347 K. Since initial water saturation can decrease due to wettability alteration, the cores containing water (#2 and #4) were flooded again with oil after the aging period.

Fig. 1 shows the system for the fluid saturation of cores at reservoir temperature. It consists of two containers for oil and RB, a core holder, a manual pump to adjust the overburden pressure, a pressure gauge, a differential pressure gauge, fluid collectors, and an oven. For cores #2 and #4, oil was injected into the cores at 100 cm^3/hr until no water was produced.

Before each coreflooding experiment, a fracture was created for each core with an electrical saw as shown in Fig. 2. Two Teflon strips of 0.001 m in width and 0.229 m in length were placed inside the fracture to keep an aperture of the fracture. The core halves were put together with the Teflon strips between them and wrapped with a heat-shrinkable Teflon tube. This experimental procedure is based on Mejia [30]. Finally, the core was placed horizontally inside the core holder with the fracture vertically-oriented.

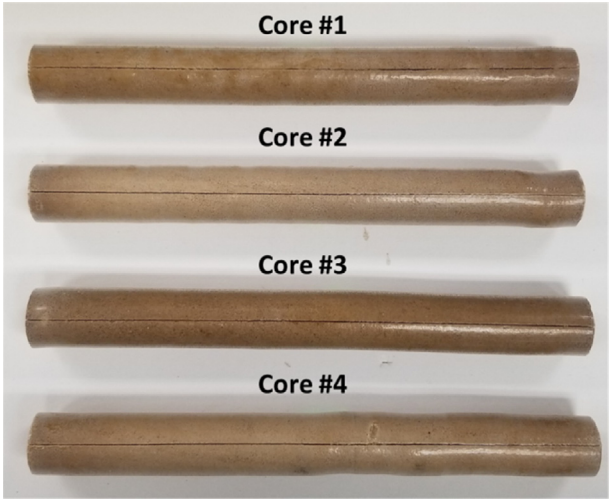

Fig. 2. Artificially fractured Texas cream limestones cores. The diameter is 0.0254 m and the length is 0.229 m. Cores #1 (S_{wi} = 0) and #2 (S_{wi} = 0.311) were used for coreflooding experiments with 3pRB, and cores #3 (S_{wi} = 0) and #4 (S_{wi} = 0.28) with 3p. Table 3 shows the properties of the fractured cores.

Table 3 provides the properties of the cores and other important parameters for the design of coreflooding experiments. Cores #1 and #2 were used for 3pRB injection, and cores #3 and #4 for pure 3p injection. Note again that cores #1 and # 3 were fully saturated with oil and cores #2 and #4 contained initial water saturations, 31.1% and 28.0%, respectively.

Fig. 3 presents a schematic of the setup for the coreflooding experiments. It consists of accumulators for crude oil, RB, and 3-pentanone (3pRB or pure 3p), a pump, a core holder, a hydraulic manual pump to maintain overburden pressure, a pressure gauge, a differential pressure gauge, fluid collectors, and an oven.

After placing a fractured core in the core holder, the oven

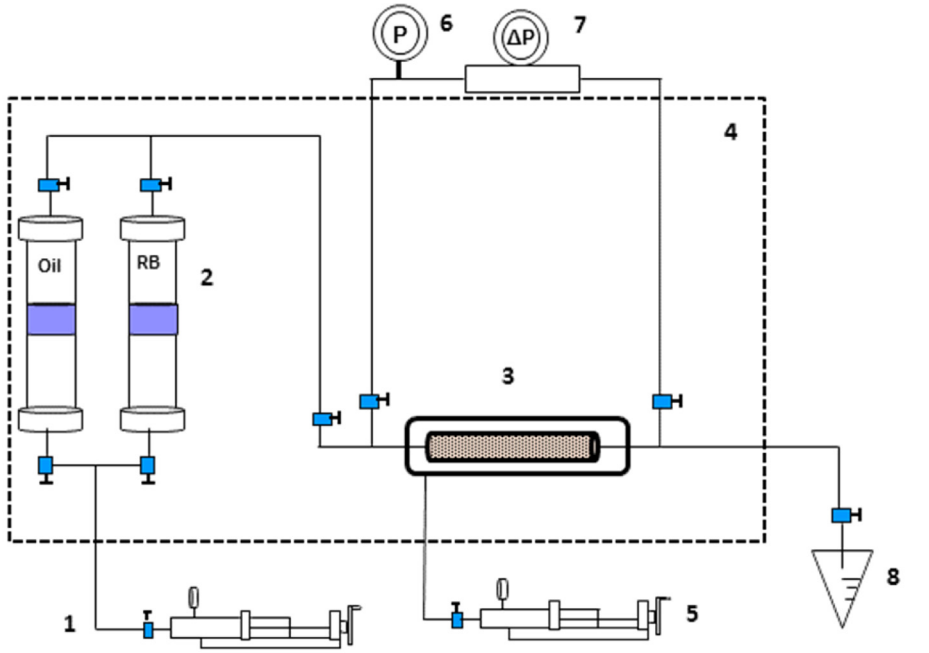

Fig. 1. Schematic of the experimental setup for saturation of cores with oil and RB (Section 2.3).

Table 3
Properties of the cores used for coreflooding experiments. Cores #1 and #2 were used for a slug injection of 1.1 wt% 3-pentanone solution in RB (3pRB). Cores #3 and #4 were used for the injection of pure 3-pentanone as a slug.

	Core #1	Core #2	Core #3	Core #4
Matrix porosity	0.274	0.280	0.286	0.280
Matrix permeability, mD	19.9	17.8	31.6	17.8
Matrix water saturation	0.0	0.311	0.0	0.280
Matrix oil saturation	1.0	0.689	1.0	0.720
Flow capacity of the matrix, m^4	9.947×10^{-18}	8.901×10^{-18}	1.580×10^{-17}	8.901×10^{-18}
Mass of the core before cutting, kg	0.25056	0.25191	0.2465	0.25018
Mass of the core after cutting, kg	0.23000	0.23227	0.2263	0.2293
Matrix pore volume after cutting, m^3	2.909×10^{-5}	3.005×10^{-5}	3.034×10^{-5}	2.969×10^{-5}
Pressure drop along the core at 100 cm^3/hr, kPa	6.895	10.689	3.654	8.274
Overburden pressure, kPa	2068	2068	7584	6550
Fracture aperture, m	1.03×10^{-4}	9.72×10^{-5}	1.28×10^{-4}	9.74×10^{-5}
Fracture permeability, D	900	798	1398	801.7
Permeability contrast between fracture and matrix	45,249	44,831	44,241	45,039
Flow capacity of fracture, m^4	2.330×10^{-15}	1.944×10^{-15}	4.509×10^{-15}	1.958×10^{-15}
Fracture pore volume, m^3	6×10^{-7}	5.6×10^{-7}	7.5×10^{-7}	5.6×10^{-7}
Total pore volume, m^3	2.97×10^{-5}	3.06×10^{-5}	3.11×10^{-5}	3.03×10^{-5}

temperature was set to reservoir temperature (347 K). Then, oil was injected to remove any air inside the fracture and tubing. Oil flow rate was gradually increased from 20 to 1000 cm^3/hr. A partially-closed valve was placed at the outlet of the system to maintain the fracture space filled out with liquid. This also kept the outlet pressure slightly higher than the atmospheric pressure. Fracture permeability was measured using a flow rate of 100 cm^3/hr. The overburden pressure was regulated to make the fracture/matrix permeability ratio within the range between 63,634 and 33126. This range was calculated from available data of fracture conductivity, fracture width, and matrix permeability for shale plays [31–33]. The permeability ratio was set to be similar to that in shales.

The fracture permeability, k_f, was obtained by the method described by Mejia [30]. The fracture aperture was obtained from the equation for flow between parallel plates:

$$b = (3\pi d k_e)^{\frac{1}{3}} \quad (1)$$

where b is the fracture aperture, d is the core diameter, and k_e is the effective oil permeability of the fractured core from Darcy's law. The fracture permeability was then estimated from the fracture aperture by the following equation:

$$k_f = b^2/12 \quad (2)$$

Table 3 provides the pressure drops along the cores at 100 cm^3/hr, the overburden pressures, the fracture apertures, the fracture permeabilities and the fracture/matrix permeability ratios (permeability contrasts). The flow capacities of the fracture (k_fA_f) and the matrix (k_mA_m) are also shown in Table 3. A_f and A_m are cross-sectional areas of the fracture and matrix. K_f and k_m are permeabilities of the fracture and matrix. The flow capacities of the fractures were approximately 240 times greater than those of the matrix.

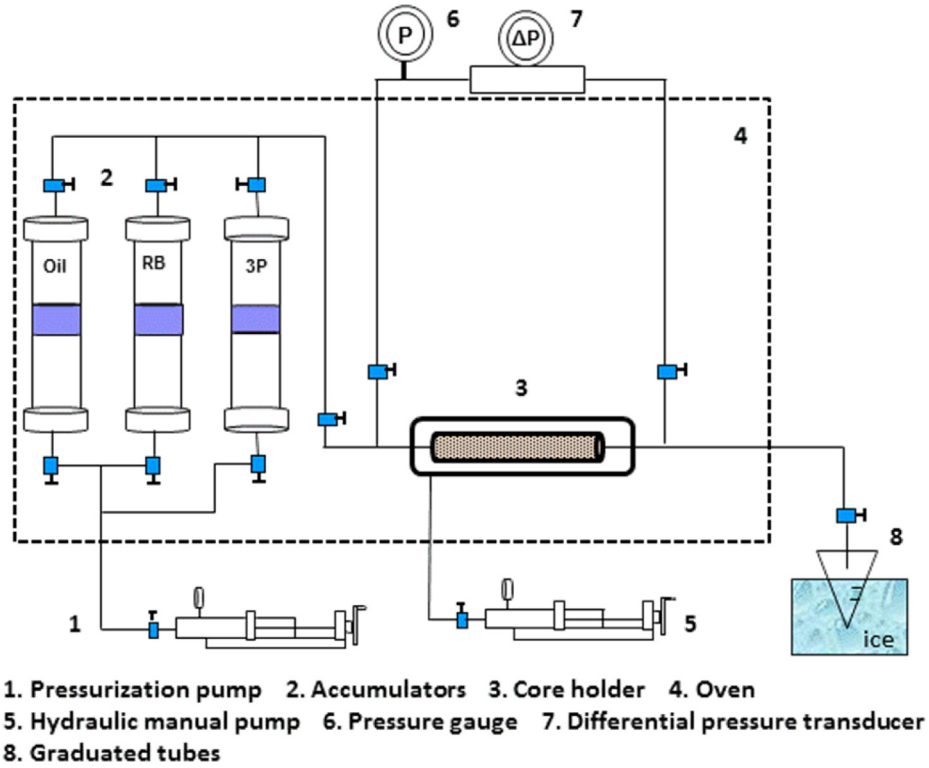

Fig. 3. Schematic of the experimental setup for coreflooding experiments (Section 2.3).

The coreflooding experiments were performed at 347 K with an injection scheme consisting of three stages: the first stage with RB with no chemical, the second stage with a chemical slug (either 3pRB or pure 3p), and the third stage with "chase" RB. The RB for the initial stage was injected at 6 cm^3/hr until no oil production was observed. For the second stage, the chemical slug, either 3pRB or pure 3p, was injected at a flow rate based on 1 h of residence time in the fracture. Finally, the chase RB was injected at the same flow rate calculated for the chemical slug until there was no more oil production for cores #1 and #3. For cores #2 and #4, however, the RB injection was stopped after 4.3 PVI.

The produced fluids were collected in plastic graduated tubes. The 3-pentanone concentrations in the oleic and aqueous phases were measured by the ^{1}H NMR method for the chemical slug and chase RB periods for all cores. The concentration data were used to correct oil-recovery results for 3-pentanone solubility, and to analyze the material balance for each coreflooding. The tubes were placed in an ice bath to avoid evaporation of 3p for cores #3 and #4 after the excessive vaporization of 3p was noticed for corefloods with cores #1 and #2.

The flow rate of the chemical slug (3pRB or pure 3p) was designed to set the chemical residence time to approximately 1 h. The residence time in the fracture, τ, is

$$\tau = V_f/q \tag{3}$$

where V_f is the volume of fracture, and q is the flow rate of the chemical slug in the fracture. Table 4 summarizes the coreflooding experiments in this research and shows the flow rates during the injection of the chemical slug. As noted previously, the chemical slug was 3pRB for cores #1 (S_{wi} = 0) and #2 (S_{wi} = 0.311), and pure 3p for cores #3 (S_{wi} = 0) and #4 (S_{wi} = 0.280). To analyze the effects of S_{wi} on oil recovery and imbibition, core #1 was compared to core #2 for 3pRB, and core #3 to core #4 for pure 3p.

2.4. Material balance for a fractured core

Analysis of the coreflooding results requires the material balance analysis for (pseudo)components, brine, oil, and 3p. Since oil recovery in this research occurs by replacing oil with brine and/or 3p in the matrix pore volume, it is important to estimate how much of injected components was imbibed into the matrix from the fracture. The material balance is also useful in estimating the relative contribution of brine and 3p to displacing oil from the matrix pore volume.

The material balance for (pseudo)component i (i = 1 for brine, 2 for oil, and 3 for 3p) for the horizontal flooding with a vertically-oriented fracture (Fig. 4) is based on the following assumptions:

- The system volume consists of two subvolumes, the fracture volume (V_f) and the matrix volume (V_m).
- The fracture volume is connected to the injector (source) and the producer (sink).
- The system is closed except for the injector and producer.
- No chemical reaction.

For a given time interval Δt,

$$\Delta M_{fi} = M_{ti} + M_{Ii} + M_{Pi} \tag{4}$$

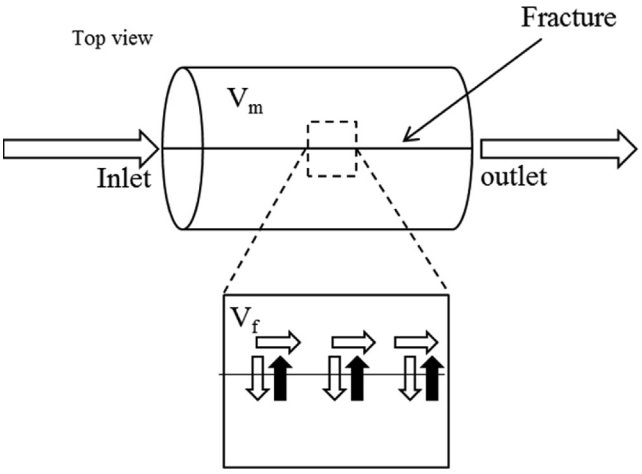

Fig. 4. Schematic of the dynamic imbibition from a fracture into a matrix for the material balance in the coreflooding experiments (Section 2.3). The figure shows the top view of a horizontally placed core with a vertically-oriented fracture along the core. V_m is the matrix volume; V_f is the fracture volume.

$$\Delta M_{mi} = -M_{ti} \tag{5}$$

where ΔM_{fi} and ΔM_{mi} are the accumulation of component i in V_f and V_m, respectively. M_{Ii} is the amount of component i going into V_f through the injector for Δt, M_{Pi} is the amount of component i going into V_f through the producer for Δt, and M_{ti} is the amount of component i transferred from V_m to V_f through the matrix/fracture interface for Δt. Note again that i = 1 for brine, 2 for oil, and 3 for 3p.

When this material balance is applied to the time interval Δt, during which flow in V_f is at steady state, ΔM_{fi} are zero for all i. Since M_{Ii} and M_{Pi} are known for all i for the corefloods (M_{I2} = 0, in particular), M_{ti} and, therefore, ΔM_{mi} are given for all i. The M_{ti} values so calculated are net amounts because the gross amounts of mass transfer between V_m and V_f for Δt are unknown in general.

How much of the injected amount is actually imbibed into V_m is quantified by the imbibed fraction for component i (F_i). This imbibed fraction is an "apparent" value because M_{ti} is the net amount of mass transfer from V_m to V_f as mentioned previously. The apparent imbibed fraction for component i, F_i, is defined for Δt as

$$F_i = -M_{ti}/M_{Ii} \tag{6}$$

F_1 and F_3 are calculated from the experimental data and used to interpret the imbibition experiments of this research.

Furthermore, the contributions of brine (i = 1) and 3p (i = 3) to displacing oil (i = 2) in the matrix are estimated by assuming no volume change on mixing of 3p and brine, and 3p and oil for the volume balance for V_m. That is, $\sum_{i=1}^{3} V_{ti} = 0$, and therefore $\sum_{i=1}^{3} (V_{Ii} + V_{Pi}) = 0$, where V_{ti} is the volume of component i transferred from V_m to V_f through the matrix/fracture interface for Δt, V_{Ii} is the volume of component i going into V_f through the injector for Δt, and V_{Pi} is the volume of component i going into V_f through the producer for Δt. Then, the produced oil for Δt is expressed as

$$-V_{P2} = (V_{I1} + V_{P1}) + (V_{I3} + V_{P3}) \tag{7}$$

Table 4
Summary of the coreflooding experiments. Cores #1 and #2 were used for the slug injection of 1.1- wt% 3-pentanone solution in RB (3pRB). Cores #3 and #4 were used for the slug injection of pure 3-pentanone. τ is the residence time of the chemical product (3pRB or 3p) in the fracture, and q is the flow rate at which the chemical product is injected.

Core #1	Core #2	Core #3	Core #4
S_{wi} = 0 Scheme: RB/3pRB/Chase RB τ = 1 h q = 5.97 × 10^{-7} m^3/hr	S_{wi} = 0.311 Scheme: RB/3pRB/Chase RB τ = 1 h q = 5.62 × 10^{-7} m^3/hr	S_{wi} = 0 Scheme: RB/3p/Chase RB τ = 1 h q = 7.45 × 10^{-7} m^3/hr	S_{wi} = 0.28 Scheme: RB/3p/Chase RB τ = 1 h q = 5.64 × 10^{-7} m^3/hr

The contribution of component i to displacing oil from the matrix, D_i, is defined as

$$D_i = -(V_{Ii} + V_{Pi})/V_{P2} \quad (8)$$

for i = 1 and 3. Note that $D_1 + D_3 = 1.0$

3. Results and discussion

This section presents the main results of the coreflooding experiments with 3pRB (cores #1 and #2) and pure 3p (cores #3 and #4) in separate subsections. As presented in Section 2.4, the mass/volume balance equations give F_i and D_i for i = 1 and 3, and the resulting oil recovery results are discussed. Since brine (i = 1) was not injected into cores #3 and #4, the discussion is centered on the effects of S_{wi} on F_3 in Section 3.2.

The main focus of the coreflooding is on the effect of S_{wi} on the displacement of oil (i = 2) by brine (i = 1) and/or 3p (i = 3) through the fracture/matrix interface. The effects of S_{wi} on water imbibition have been studied for conventional reservoirs, but no detailed analysis of material balance has been presented in the literature.

3.1. Coreflooding experiments with 3pRB for cores #1 and #2

Fig. 5a shows the oil recovery factors for cores #1 (S_{wi} = 0) and #2 (S_{wi} = 0.311). As mentioned in Section 2.3, RB was first injected into the cores until no more oil production was observed. Then, 3pRB was injected to improve the oil recovery for approximately 1.0 pore-volume injected (PVI). After that, the chase RB was injected until the water cut becomes essentially 100%. The chase RB injection was terminated at 0.84 PVI for core #1 and 2.11 PVI for core #2.

The initial RB injection showed that the oil recovery factor was clearly higher for core #2 than for core #1. The final recovery factor for this initial RB injection was 9.8% after 0.7 PVI for core #1, and 15.1% after 0.5 PVI for core #2. This indicates that the RB imbibition rate was more rapid for core #2 despite the fact that core #1 had a slightly higher permeability than core #2 (Table 3). The initial phase distribution likely affected the RB imbibition into these cores.

The incremental oil recovery factor during the 3pRB slug injection was 3.2% for core #1, and 7.3% for core #2. The imbibition was more rapid for core #2 as was the case with the initial RB injection.

The chase RB injection reached the ultimate oil recovery factor for core #1, with an incremental oil recovery factor of 0.3% after only 0.17 PVI. The chase RB injection was continued until 0.84 PVI for core #1. For core #2, however, the chase RB injection did not reach a plateau until it was terminated at 2.11 PVI. This chase RB injection yielded an incremental oil recovery factor of 5.3% for core #2, which is much greater than 0.3% for core #1.

The total oil recovery factor after the three stages was 13.3% for core #1, and 27.7% for core #2. It is clearly shown that 3pRB increased oil recovery beyond what the RB injection could recover; that is, the rock wettability should have changed to more water-wet, especially for core #2. The results indicate that the injected 3p was more efficiently used for enhancing the imbibition of brine (i = 1) for core #2 than for core #1 as explained below.

Li et al. showed that, in addition to rock properties, the unit used for oil recovery affected the interpretation of imbibition experiments [34]. Fig. 5b presents the oil recovery in the unit of pore volume (PV) for cores #1 and #2. The trends of oil recovery, imbibition rate, and the effectiveness of 3pRB for these cores are consistent with the observations made for Fig. 5a.

Figs. 6 and 7 show the oil recovery (in PV), F_1, and F_3 for cores #1 and #2, respectively. The calculation of F_i was done separately for the three stages; e.g., the time interval for F_i for the 3pRB stage starts upon the commencement of the 3pRB injection. After the 3pRB injection, F_3 was 0.738 for both cores #1 and #2. It remained high during the 3pRB injection for both cores; that is, the effect of S_{wi} on F_3 was not observed.

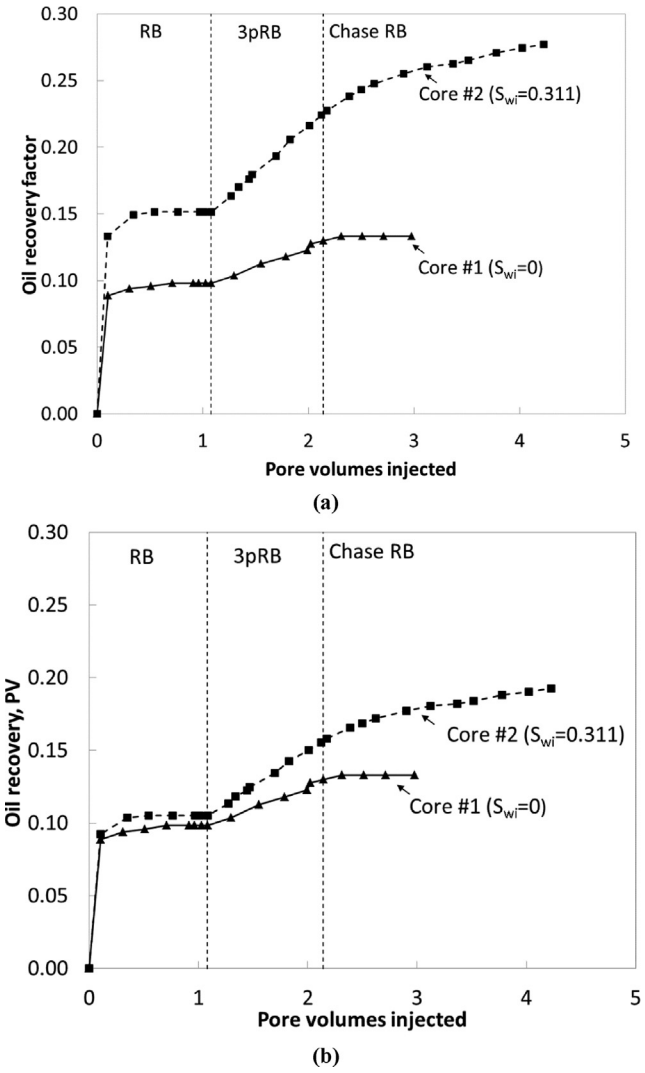

Fig. 5. (a) Oil recovery factors (in the unit of OOIP) during coreflooding experiments at 347 K using 3pRB as the chemical slug. (b) Oil recovery in PV during coreflooding experiments at 347 K using 3pRB as the chemical slug. First, RB was injected into Cores #1 (S_{wi} = 0) and #2 (S_{wi} = 0.311) until no more oil production was observed. Then, 3pRB was injected for 1 PVI. Finally, chase RB was injected. The injection of chase RB was terminated for core #1 after 0.84 PVI, for core #2 after 2.11 PVI. RB, 3pRB, and S_{wi} stand for reservoir brine, solution of 1.1- wt% 3p in reservoir brine, and initial water saturation, respectively.

However, F_1 was 0.018 for core #1, and 0.038 for core #2; that is, F_1 was larger with the larger S_{wi}.

For the chase RB stage, F_1 was 0.004 for core #1, and 0.018 for core #2. Note that the RB imbibition continued to occur when the chase RB injection was terminated for core #2. The presence of S_{wi} was conducive to enhancement of F_1 by the imbibed 3p both for the 3pRB and RB injection stages.

Figs. 8 and 9 show the volume of produced oil, and the volumes of oil displaced by RB and 3p from the matrix to the fracture. These parameters were calculated on the cumulative basis, for which the time interval started at 0 PVI across all three stages. D_i was also calculated on a cumulative basis, for which the time interval started upon the commencement of the 3pRB injection. During the 3pRB injection, D_1 was 61% for core #1, but it was as large as 77% for core #2 (see Eq. (8) in Section 2.4). This reconfirms that 3-pentanone is more effective for enhancing the imbibition of brine by wettability alteration when an aqueous phase is initially present in the matrix. When the 3pRB and

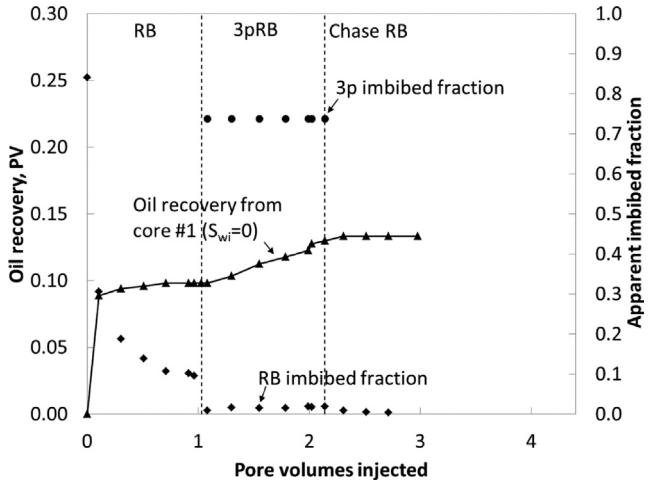

Fig. 6. Oil recovery in pore volume units (left vertical axis) and apparent imbibition of RB and 3-pentanone (right vertical axis) during the coreflooding experiment at 347 K using 3pRB as the chemical slug, for core # 1 (S_{wi} = 0). RB, 3pRB, 3p, and S_{wi} stand for reservoir brine, solution of 3p in reservoir brine, 3-pentanone, and initial water saturation, respectively.

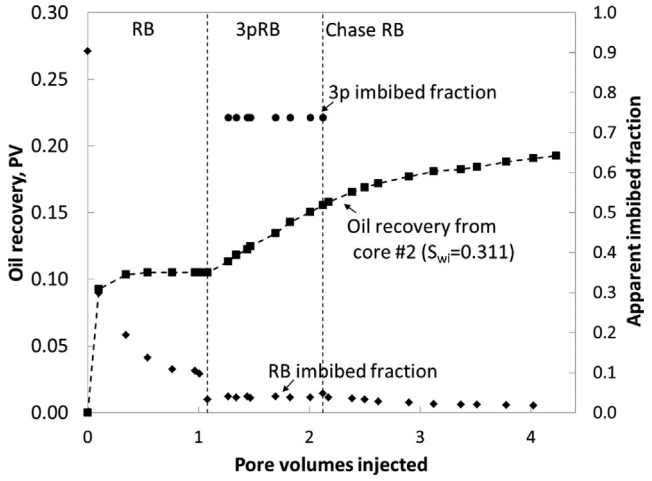

Fig. 7. Oil recovery in PV (left vertical axis) and the apparent imbibed fractions of RB and 3-pentanone (right vertical axis) during the coreflooding experiment at 347 K using 3pRB as the chemical slug for core # 2 (S_{wi} = 0.311). RB, 3pRB, 3p, and Swi stand for reservoir brine, solution of 1.1- wt% 3p in reservoir brine, 3-pentanone, and initial water saturation, respectively.

chase RB injection are both considered, D_1 was 65% for core #1 and 87% for core #2, and it was increasing further when the experiment was terminated for core #2.

3.2. Coreflooding experiments with pure 3p for cores #3 and #4

Fig. 10 presents the oil recovery results for cores #3 (S_{wi} = 0) and #4 (S_{wi} = 0.28), for which pure 3p was tested as a chemical slug. The oil recovery in Fig. 10a is given in the unit of original oil in place (OOIP), and that in Fig. 10b is in PV. As was done for the other cores, the initial RB injection was continued until no more oil production was observed. Then, a slug of pure 3p was injected to improve the oil recovery. Note that pure 3p is miscible with oil, and the solubility of water in 3p is approximately 3 wt% at 343 K [18,35]. After that, the chase RB injection was continued until no more oil production was observed. The chase RB injection was concluded after 1.11 and 1.97 PVI for cores #3 and #4, respectively.

The initial RB injection recovered 12% OOIP after 0.71 PVI for core #3, and 14% OOIP after 0.49 PVI for core #4. Note that core #3 was

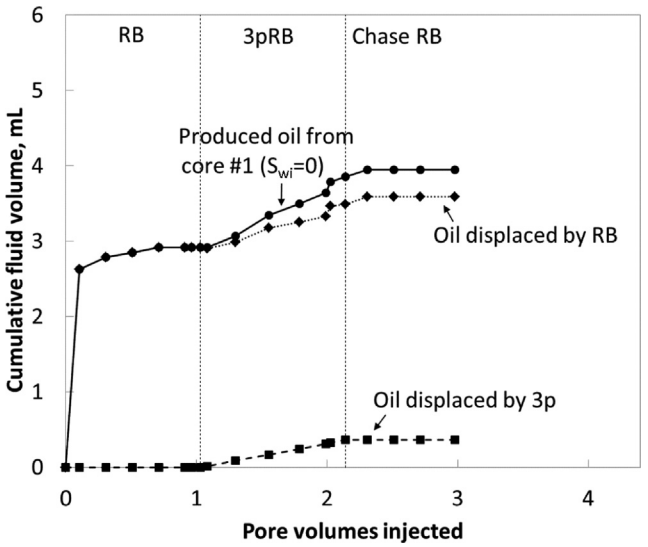

Fig. 8. Cumulative volume of produced oil, and the volumes of oil from the matrix displaced by RB and 3p in core #1 (S_{wi} = 0) for the coreflooding experiment at 347 K using 3pRB as the chemical slug. RB, 3pRB, 3p, and S_{wi} stand for reservoir brine, solution of 1.1- wt% 3p in reservoir brine, 3-pentanone, and initial water saturation, respectively.

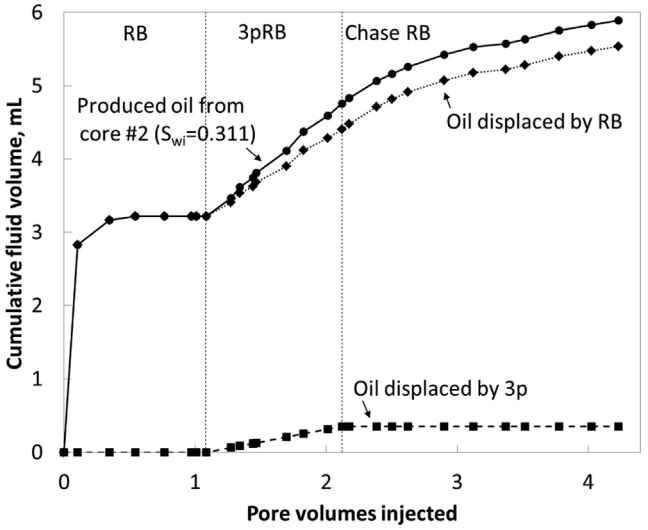

Fig. 9. Cumulative volume of produced oil, and the volumes of oil from the matrix displaced by RB and 3p in core #2 (S_{wi} = 0.311) for the coreflooding experiment at 347 K using 3pRB as the chemical slug. RB, 3pRB, 3p, and S_{wi} stand for reservoir brine, solution of 1.1- wt% 3p in reservoir brine, 3-pentanone, and initial water saturation, respectively.

clearly more permeable than core #4 as given in Table 3 (31.6 mD in comparison to 17.8 mD), but their porosities were quite similar to each other. The oil recovery in PV (Fig. 10b) shows that the initial RB injection recovered a larger amount of oil from core #3.

Fig. 10 shows that the incremental oil recovery by the 3p slug was 50.5% OOIP (50.5% PV) for core #3 and 78.1% OOIP (56.5% PV) for core #4. The chase RB injection reached a plateau with an incremental oil recovery of 1.1% OOIP after 0.36 PVI for core #3. It recovered an incremental oil of 3.7% OOIP after 1.97 PVI for core #4. No plateau was observed before the experiment was terminated for core #4 as shown in Fig. 10. The total oil recovery was 63.2% OOIP (63.2% PV) for core #3, and 95.6% OOIP (69.1% PV) for core #4.

Figs. 11 and 12 present the oil recovery (PV), F_1, and F_3 for cores #3 (S_{wi} = 0) and #4 (S_{wi} = 0.28), respectively. For core #3, F_3 was 0.550 after 1.0 PVI. As in the previous subsection, the calculation of F_i was

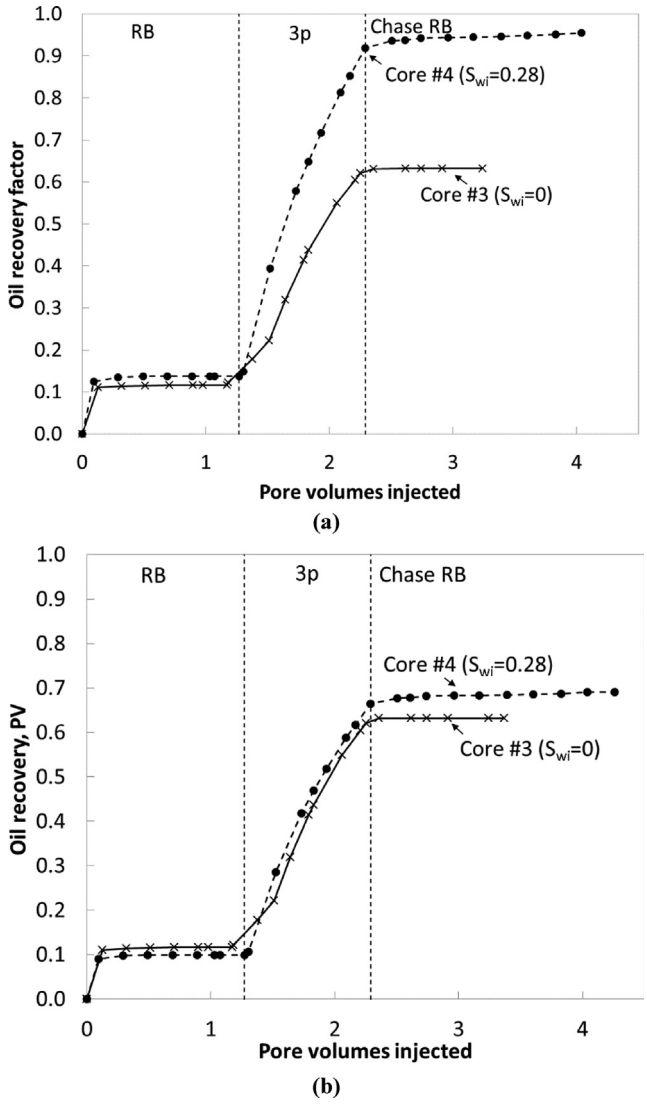

Fig. 10. (a) Oil recovery factors (in the unit of OOIP) during coreflooding experiments at 347 K using 3p as the chemical slug. (b) Oil recovery in PV during coreflooding experiments at 347 K using 3p as the chemical slug. First, RB was injected into cores #3 (S_{wi} = 0) and #4 (S_{wi} = 0.28) until no more oil production was observed. Then, 3p was injected for 1 PVI. Finally, chase RB was injected. The injection of chase RB was terminated for core #3 after 1.11 PVI, for core #4 after 1.97 PVI. RB, 3p, and S_{wi} stand for reservoir brine, 3-pentanone, and initial water saturation, respectively.

done separately for the three stages: the initial RB, the 3p slug, and the chase RB injection. That is, the time interval, Δt, for the calculation was defined for each stage independently.

For core #4, F_3 was 0.601 after 1.0 PVI. That is, F_3 was measured to be larger with the presence of initial water in the matrix. 3-pentanone in the aqueous phase changed the wettability of the rock surface during the 3p displacement. F_1 during the chase RB injection reached a maximum value of 0.274 after 0.10 PVI, and then rapidly decreased to 0.030 after 1.11 PVI for core #3. For core #4, F_1 showed a maximum value of 0.112 after 0.22 PVI, and then decreased to 0.025 after 1.97 PVI.

Figs. 13 and 14 show the volume of produced oil and the volumes of RB and 3p transferred from fracture to matrix for cores #3 and #4, respectively. As in the previous subsection, the time interval for this calculation starts at the beginning of the initial RB injection. They clearly show that the oil recovery from the matrix relied more on oil displacement by 3-pentanone (i = 3) than by brine (i = 1) during the

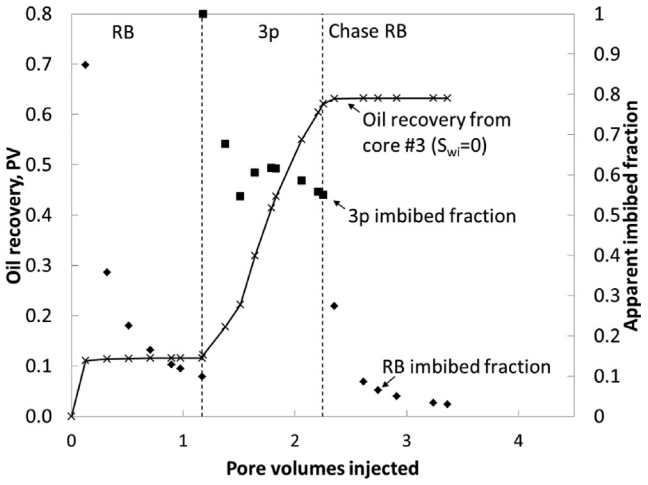

Fig. 11. Oil recovery in pore volume units (left vertical axis) and apparent imbibition of RB and 3p (right vertical axis) during the coreflooding experiment at 347 K using 3p as the chemical slug, for core # 3 (S_{wi} = 0). RB, 3p, and S_{wi} stand for reservoir brine, 3-pentanone, and initial water saturation, respectively.

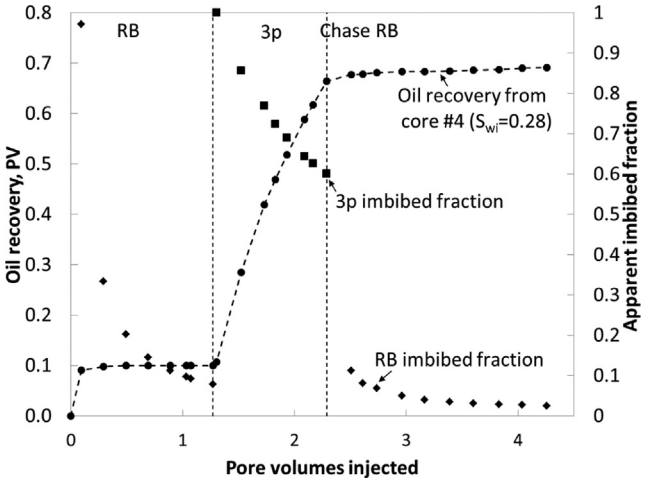

Fig. 12. Oil recovery in pore volume units (left vertical axis) and apparent imbibition of RB and 3p (right vertical axis) during the coreflooding experiment at 347 K using 3p as the chemical slug, for core # 4 (S_{wi} = 0.28). RB, 3p, and S_{wi} stand for reservoir brine, 3-pentanone, and initial water saturation, respectively.

3p slug injection.

4. Conclusions

This paper presented a new set of coreflooding data with fractured carbonate cores for investigation of the improved oil recovery by injection of 3pRB (cores #1 and 2) and pure 3p (cores #3 and 4) as a slug. The experimental results were analyzed in detail in terms of material balance (mass and volume) with simplifying assumptions. This analysis enabled to estimate how much of the injected components were imbibed into the matrix from the fracture (F_1 and F_3 in Section 2.4) and the relative contribution of the injected components to displacing oil in the matrix (D_1 and D_3 in Section 2.4). The main focus of the corefloods was on the effect of the presence of an initial aqueous phase on oil recovery by using 3pRB or pure 3p. Conclusions are as follows:

1. The injection of 3pRB led to an incremental oil recovery after the RB injection reached a plateau in oil recovery for cores #1 and 2. The improved oil recovery was caused by the efficient imbibition of 3-

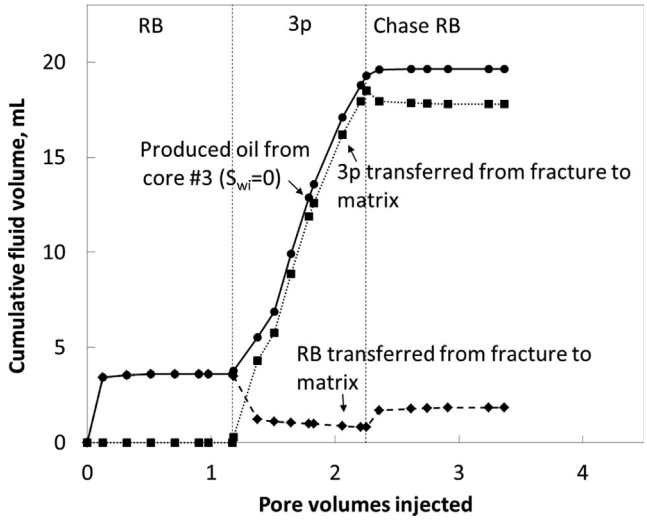

Fig. 13. Cumulative volume of produced oil, and the volumes of RB and 3p that transferred from fracture to matrix in core #3 (S_{wi} = 0) for the coreflooding experiment at 347 K using 3p as the chemical slug. RB, 3p, and S_{wi} stand for reservoir brine, 3-pentanone, and initial water saturation, respectively.

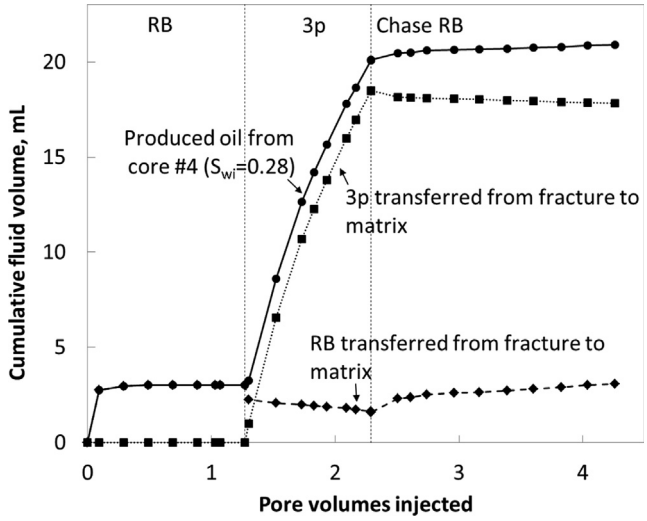

Fig. 14. Cumulative volume of produced oil, and the volumes of RB and 3p that transferred from fracture to matrix in the core #4 (S_{wi} = 0.28) for the coreflooding experiment at 347 K using 3p as the chemical slug. RB, 3p, and S_{wi} stand for reservoir brine, 3-pentanone, and initial water saturation, respectively.

pentanone into the matrix, resulting in enhanced water imbibition by the wettability alteration.

2. The oil recovery for core #2 (S_{wi} = 0.311) was consistently greater than that of core #1 (S_{wi} = 0) in both units of OOIP and PV. The total oil recovery factor was 27.7% OOIP (19.2% PV) for core #2, and 13.3% OOIP (13.3% PV) for core #1.
3. The total oil recovery was 63.2% OOIP (63.2% PV) for core #3 (S_{wi} = 0) and 95.6% OOIP (69.1% PV) for core #4 (S_{wi} = 0.28). The incremental oil recovery during the 3p injection was 50.5% OOIP (50.5% PV) for core #3, and 78.1% OOIP (56.5% PV) for core #4. Although core #4 contained a smaller amount of oil in the matrix, it produced more oil from core #4 than from core #3 with the pure 3p injection followed by the chase RB injection.
4. F_3 was estimated to be 0.74 for both cores #1 and #2 during the 3pRB injection. F_3 was not significantly affected by the presence of the initial aqueous phase in the matrix for the 3pRB cases (cores #1 and #2).
5. F_3 was estimated to be 0.55 for core #3 and 0.60 for core #4 during the 3p injection. The transfer of 3-pentanone from the fracture to the matrix was more efficient with the presence of an initial aqueous phase in the matrix.
6. F_1 was estimated to be 0.018 for core #1 and 0.038 for core #2 during the 3pRB injection. It was clearly greater when an aqueous phase was initially present in the matrix. F_1 in the chase RB injection stage was also greater for core #2 (0.018) than for core #1 (0.004).
7. D_1 was estimated to be 61% for core #1 and 77% for core #2 during the 3pRB injection stage. It was 65% for core #1 and 87% for core #2 when the 3pRB and chase RB injection stages are considered. This clearly shows that 3-pentanone was more effective in enhancing the water imbibition when an aqueous phase was initially present in the matrix.
8. The coreflooding results collectively showed that the injection of 3-pentanone (as either 3pRB or pure 3p) was more effective for oil recovery from the matrix when an aqueous phase was initially present in the matrix.

CRediT authorship contribution statement

Francisco J. Argüelles-Vivas: Methodology, Validation, Formal analysis, Investigation, Data curation, Writing - original draft, Visualization. **Mingyuan Wang:** Methodology, Validation, Formal analysis, Investigation, Data curation, Visualization. **Gayan A. Abeykoon:** Methodology, Validation, Formal analysis, Investigation, Data curation, Visualization. **Ryosuke Okuno:** Conceptualization, Methodology, Validation, Formal analysis, Resources, Writing - original draft, Writing - review & editing, Supervision, Project administration, Funding acquisition.

Declaration of Competing Interest

The authors declare that they have no known competing financial interests or personal relationships that could have appeared to influence the work reported in this paper.

Acknowledgements

Ryosuke Okuno holds the Pioneer Corporation Faculty Fellowship in Petroleum Engineering at The University of Texas at Austin.

References

[1] Alharthy, N., Teklu, T., Kazemi, H., Graves, R., Hawthorne, S., Braunberger, J., and Kurtoglu, B. 2015. Enhanced Oil Recovery in Liquid-Rich Shale Reservoirs: Laboratory to Field. Presented at SPE Annual Technical Conference and Exhibition, Houston, Texas, USA, 28-30 September. SPE-175034-MS. http://dx.doi.org/10.2118/175034-MS.

[2] Barba, R. E. 2015. Liquids Rich Organic Shale Recovery Factor Application. Presented at SPE Annual Technical Conference and Exhibition, Houston, Texas, USA, 28-30 September. SPE-174994-MS. http://dx.doi.org/10.2118/174994-MS.

[3] Morsy, S., Sheng, J. J., and Soliman, M. Y. 2013. Waterflooding in the Eagle Ford Shale Formation: Experimental and Simulation Study. Presented at SPE Unconventional Resources Conference and Exhibition-Asia Pacific, Brisbane, Australia, 11-13 November. SPE-167056-MS. http://dx.doi.org/10.2118/167056-MS.

[4] Alvarez JO, Schechter DS. Wettability Alteration and Spontaneous Imbibition in Unconventional Liquid Reservoirs by Surfactant Additives. SPE Reservoir Eval Eng 2017;20(01). https://doi.org/10.2118/177057-PA.

[5] Alvarez JO, Saputra IWR, Schechter DS. The Impact of Surfactant Imbibition and Adsorption for Improving Oil Recovery in the Wolfcamp and Eagle Ford Reservoirs. SPE J 2018;23(06):2103–17. SPE-187176-PA. 10.2118/187176-PA.

[6] Alvarez, J. O., Tovar, F. D., and Schechter, D. S. 2018. Improving Oil Recovery in the Wolfcamp Reservoir by Soaking/Flowback Production Schedule With Surfactant Additives. SPE Reservoir Evaluation & Engineering 21(04): 1083-1096. SPE-187483-PA. http://dx.doi.org/10.2118/187483-PA.

[7] Shuler, P. J., Tang, H., Lu, Z., and Tang, Y. 2011. Chemical Process for Improved Oil Recovery from Bakken Shale. Presented at Canadian Unconventional Resources Conference, Calgary, Alberta, Canada, 15-17 November. SPE-147531-MS. http://dx.doi.org/10.2118/147531-MS.

[8] Wang D, Butler R, Zhang J, Seright R. Wettability survey in bakken shale with

surfactant-formulation imbibition. SPE Reservoir Eval Eng 2012;15(06):695–705. https://doi.org/10.2118/153853-PA. SPE-153853-PA.
[9] Kathel P, Mohanty KK. Wettability alteration in a tight oil reservoir. Energy Fuels 2013;27(11):6460–8.
[10] Alvarez, J. O., Neog, A., Jais, A., and Schechter, D. S. 2014. Impact of Surfactants for Wettability Alteration in Stimulation Fluids and the Potential for Surfactant EOR in Unconventional Liquid Reservoirs. Presented at SPE Unconventional Resources Conference, The Woodlands, Texas, USA, 1-3 April. SPE-169001-MS. http://dx.doi.org/10.2118/169001-MS.
[11] Nguyen, D., Wang, D., Oladapo, A., Zhang, J., Sickorez, J., Butler, R., and Mueller, B. 2014. Evaluation of Surfactants for Oil Recovery Potential in Shale Reservoirs. Presented at SPE Improved Oil Recovery Symposium, Tulsa, Oklahoma, USA, 12-16 April. SPE-169085-MS. http://dx.doi.org/10.2118/169085-MS.
[12] Alfarge, D., Wei, M., and Bai, B. 2017. IOR Methods in Unconventional Reservoirs of North America: Comprehensive Review. Presented at SPE Western Regional Meeting, Bakersfield, California, USA, 23-27 April. SPE-185640-MS. http://dx.doi.org/10.2118/185640-MS.
[13] Zeng, T., Miller, C. S., and Mohanty, K. K. 2018. Application of Surfactants in Shale Chemical EOR at High Temperatures. Presented at the SPE Improved Oil Recovery Conference, Tulsa, Oklahoma, USA, 14-18 April. SPE-190318-MS. http://dx.doi.org/10.2118/190318-MS.
[14] Liu J, Sheng JJ, Wang X, Ge H, Yao E. Experimental study of wettability alteration and spontaneous imbibition in chinese shale oil reservoirs using anionic and non-ionic surfactants. J Petrol Sci Eng 2019;175:624–33.
[15] Adibhatla B, Mohanty KK. Parametric analysis of surfactant-aided imbibition in fractured carbonates. J Colloid Interface Sci 2008;317(02):513–22. https://doi.org/10.1016/j.jcis.2007.09.088.
[16] Lu J, Britton C, Solairaj S, Liyanage PJ, Kim DH, Adkins S, et al. Novel large-hydrophobe alkoxy carboxylate surfactants for enhanced oil recovery. SPE J 2014;19(06):1024–34. https://doi.org/10.2118/154261-PA.
[17] Wang M, Abeykoon GA, Argüelles-Vivas FJ, Okuno R. Ketone solvent as a wettability modifier for improved oil recovery from oil-wet porous media. Fuel 2019;258:116–95. https://doi.org/10.1016/j.fuel.2019.116195.
[18] Wang M, Baek K, Abeykoon GA, Argüelles-Vivas FJ, Okuno R. Comparative study of ketone and surfactant for enhancement of water imbibition in fractured porous media. Energy and Fuels 2019;23:2019. https://doi.org/10.1021/acs.energyfuels.9b03571.
[19] Rassenfoss, S. 2018. Rising Tide of Produced Water Could Pinch Permian Growth. Journal of Petroleum Technology. https://pubs.spe.org/en/jpt/jpt-article-detail/?art=4273.
[20] Viksund, B. G., Morrow, N. R., Ma, S., Wang, W., and Graue, A. 1998. Initial water saturation and oil recovery from chalk and sandstone by spontaneous imbibition. Paper SCA-9814, proceedings of the International Symposium of the Society of Core Analysts, the Hague, Netherlands, 14-16 September.
[21] Cil, M., Reis, J. C., Miller, M. A., and Misra, D. 1998. An Examination of Countercurrent Capillary Imbibiton Recovery from Single Matrix Blocks and Recovery Predictions by Analytical Matrix/fracture Transfer Functions. Presented at the SPE Annual Technical Conference and Exhibition, New Orleans, Lousiana, USA, 27-30 September. SPE-49005-MS. https://doi.org/10.2118/49005-MS.
[22] Zhou X, Morrow NR, Ma S. Interrelationship of wettability, initial water saturation, aging time, and oil recovery by spontaneous imbibition and waterflooding. SPE J 2000;5(2):199–207. https://doi.org/10.2118/62507-PA. SPE-62507-PA.
[23] Akin S, Schembre JM, Bhat SK, Kovscek AR. Spontaneous imbibition characteristics of diatomite. J Petrol Sci Eng 2000;25:149–65. https://doi.org/10.1016/S0920-4105(00)00010-3.
[24] Tong, Z., Xie, X., Morrow, N. R. 2001. Scaling of Viscosity Ratio for Oil Recovery by Imbibition from Mixed-Wet Rocks. Paper SCA 2001-21, proceedings of the International Symposium of the Society of Core Analysis, Edinburgh, UK, 17-19 September.
[25] Li K, Li Y. Effect of initial water saturation on crude oil recovery and water cut in water-wet reservoirs. Int J Energy Res 2014;38:1599–607. https://doi.org/10.1002/er.3182.
[26] Ghanbari E, Dehghanpour H. Impact of rock fabric on water imbibition and salt diffusion in gas shales. Int J Coal Geol 2015;138:55–67. https://doi.org/10.1016/j.coal.2014.11.003.
[27] Gao Z, Hu Q. Initial water saturation and imbibition fluid affect spontaneous imbibition into Barnett shale samples. J Nat Gas Sci Eng 2016;34:541–51. https://doi.org/10.1016/j.jngse.2016.07.038.
[28] Bowker KA. Recent developments of the Barnett shale play. Fort Worth Basin: West Texas Geological Society Bulletin 2003;42(6):4–11. http://www.searchanddiscovery.com/documents/2007/07023bowker/.
[29] Daubert TE, Danner RP. Data compilation tables of properties of pure compounds. New York: American Institute of Chemical Engineers; 1985.
[30] Mejia, M. 2018. Experimental Investigation of Surfactant Flooding in Fractured Limestones. MS thesis, The University of Texas at Austin, Austin, Texas (December 2018).
[31] Zhang J, Kamenov A, Zhu D, Hill AD. Development of new testing procedures to measure propped fracture conductivity considering water damage in clay-rich shale reservoirs: an example of the Barnett Shale. J Petrol Sci Eng 2015;135:352–9. https://doi.org/10.1016/j.petrol.2015.09.025.
[32] Siriwardane, H., Gondle, R., Bromhal, G. 2016. Extent of Hydraulic Fractures in Shales. NETL Technical Report Series; U.S. Department of Energy, National Energy Technology Laboratory: Morgantown, WV, 2016; p 55. https://edx.netl.doe.gov/dataset/extent-of-hydraulic-fractures-in-shales.
[33] Shen Y, Pang Y, Shen Z, Tian Y, Ge H. Multiparameter analysis of gas transport phenomena in shale gas reservoirs: apparent permeability characterization. Sci Rep 2018;8:2601. https://doi.org/10.1038/s41598-018-20949-2.
[34] Li K, Chow K, Horne RN. Influence of initial water saturation on recovery by spontaneous imbibition in gas/water/rock systems and the calculation of relative permeability. SPE Reservoir Eval Eng 2006;9(04):295–301. https://doi.org/10.2118/99329-PA.
[35] Stephenson RM. Mutual solubilities: water-ketones, water-ethers, and water-gasoline-alcohols. J Chem Eng Data 1992;37:80–95. https://doi.org/10.1021/je00005a024.